HEALTH SCIENCES

Rehmannia Glutinosa Polysaccharide Regulates Bone Marrow Microenvironment via HIF-1α/NF-κB Signaling Pathway in Aplastic Anemia Mice

NA LIU, JUN-QIU LIU, YONG LIU, QING ZHU, DANDAN ZHENG, FENG LI, LING-ZHAN MENG & MIN QIU

Abstract: Aplastic anemia (AA), a rare disorder, is associated with bone marrow microenvironment (BMM). Presently, AA treatment is of great difficulty. This study aimed to explore the mechanism of action of Rehmannia glutinosa polysaccharide (RGP) in AA. Busulfan was used to induce AA in BALB/c mice; blood cell count and Ray's Giemsa staining were used to assess the severity of hematopoietic failure; HE was performed to assess the pathological state of the marrow cavity; ELISA was performed to assess IL-4, IL-10, IL-6, IL-12, IL-1β, TNF-α, MCP-1, VEGF, and EPO; and WB was performed to evaluate the effects of RGP on the HIF-1α/NF-κB signaling. Significant downregulation of hemocyte levels in the blood and nucleated cells in the bone marrow was reversed by RGP and Cyclosporine A (CA). Compared with the AA group, dilating blood sinusoids, inflammation, hematopoiesis, decreased bone marrow cells and megakaryocytes were alleviated by RGP and CA, and the HIF-1α/NF-κB signaling was inhibited too. Notably, RGP was more effective when used in combination with CA. In this study, we established a relationship between BMM and the HIF-1α/NF-κB signaling pathway and found that RGP regulates BMM by suppressing the activation of the HIF-1α/NF-κB signaling. Thus, RGP exerts a pharmacological effect on AA.

Key words: HIF-1α/NF-κB Signaling Pathway, Bone Marrow Microenvironment, 31 Aplastic Anemia, Rehmannia glutinosa polysaccharide, Cyclosporine A.

INTRODUCTION

Aplastic anemia (AA) is a rare disorder that is caused by hematopoietic failure. Bone marrow stem cells and bone marrow microenvironment (BMM) are severely damaged by physical, chemical, biological, and unknown factors (Liu & Liu 2015). Clinically, patients with AA usually have pancytopenia, bleeding, marrow fibrosis, or hypocellular bone marrow (Young 2013, Killick et al. 2016). The pathogenesis of AA is complex, but is still not fully understood. At present, AA pathogenesis might be attributed to immune damage caused by hematopoietic stem cells (HSCs) (Solomou et al. 2007, Young et al. 2010), bone marrow microenvironment failure (Young et al. 2006), impaired hematopoietic cytokine production, and cellular or humoral immunosuppression of the bone marrow (Dasouki et al. 2013).

The bone marrow microenvironment is a complex hematopoietic organ with highly vascular and adipose tissue (Polineni et al. 2020, Usmani et al. 2019). Changes in BMM have been widely described in AA patients where cells such as osteoblasts, osteoclasts, adipocytes, and MSCs, maintain the balance of BMM (Sivasubramaniyan et al. 2012). As reported, when AA occurs, the balance between lipogenic and osteogenic differentiation of bone marrow

HSCs is disrupted (Nuttall & Gimble 2004), the suppressive effect of HSCs on lymphocytes is diminished (Solomou et al. 2007), and HSCs apoptosis is increased (Li et al. 2012). Hypoxia-inducible factor 1α (HIF-1α) is a key regulator of nuclear factor kappa-B (NF-κB), and studies have shown that NF-κB is involved in inflammatory processes, oxidative stress, apoptosis, cell proliferation, and differentiation (Feng & Wu 2022). Evidence has reported that NF-κB takes part in the maintenance of BMM (Wang et al. 2016).

Rehmannia glutinosa polysaccharide (RGP) is a critical bioactive compound found in the roots of Rehmannia glutinosa (Wang & Li 1997). As studies have reported, RGP shows positive anti-cancer (Xu et al. 2017), immunoenhancement (Huang et al. 2019), hypoglycemic, and antilipidemic (Kiho et al. 1992). Rehmannia glutinosa libosch extracts have been shown to promote osteoblast differentiation (Gong et al. 2019). These results suggest that RGP may benefit the BMM of AA. Nevertheless, the function of RGP in BMM has not yet been studied. Considering the role of the HIF-1α/NF-κB signaling pathway in BMM, this study aimed to explore the effects of RGP on AA in BALB/c mice based on the HIF-1α/NF-κB signaling pathway.

MATERIALS AND METHODS

Animal model establishment

A total of 42 male BALB/c mice of 7-10 weeks of age were used to establish the AA model. Obtained from the Chengdu Da Shuo Experimental Animal Co., Ltd, China (experimental animal production license number: SYXK (Chuan)2015-030; experimental animal use permit number: SYXK (Chuan)2014-189). The mice were separated into seven groups (n=6): control, AA-A1, AA-A2, AA-A3, AA-B1, AA-B2, and AA-B3. The model was expressed as "AA", after "-", marked "A" when

mice were fed 20 mg/kg/d busulfan (Solarbio Co., Ltd, Beijing, China), marked "B" when mice were fed 40 mg/kg/d busulfan; marked "1, 2, or 3" when mice were fed busulfan for "5, 7, or 10 days". All mice were continuously fed for 10 days and saline was used for the control group. When mice were fed with busulfan for less than 10 days, they were fed an equal volume of normal saline in the remaining days. Blood samples were collected on days 1, 5, 7, and 10 and mice were sacrificed on day 10 for the experiments.

Drug treatment

Thirty male BALB/c mice of 7-10 weeks of age were used to establish the AA model. The mice were separated into five groups (n=6): control, AA, AA+RGP, AA+CA, and AA+RGP+CA. Modeling the AA by 20 mg/kg/d busulfan feeding for 10 days, next, mice were fed with 0.1 mL 500 mg/mL Rehmannia glutinosa polysaccharide (RGP) (Wuhan ChemFaces Biochemical Co., Ltd, Wuhan, China) (AA+RGP), 0.1 mL 5 mg/mL Cyclosporine A (CA) (Solarbio Co., Ltd, Beijing, China) (AA+CA) or both (AA+RGP+CA) for 10 days. Blood samples and femoral bone marrow were collected on day 10 for the experiments, and the mice were sacrificed.

Cell count

Groups (control, AA-A1, AA-A2, AA-A3, AA-B1, AA-B2, and AA-B3) of mice were sampled on days 1, 5, 7, and 10, and groups (control, AA, AA+RGP, AA+CA, AA+RGP+CA) of mice were sampled on day 10 post drug treatment. An automatic hematology analyzer (Sysmex XE 5000, Kobe, Japan) was used to measure hemoglobin (HGB), white blood cell (WBC), red blood cell (RBC), and platelet (PLT) count. Bone marrow smears were stained with Giemsa stain to count the nucleated cells.

Hematoxylin-eosin (HE) staining

The excised thighbone tissue was fixed with 10% neutral formaldehyde. Then, it was decalcified in 15% EDTA, observed for 3 days/time, and replaced with fresh 15% EDTA until decalcification was completed. The thighbone tissues were washed with PBS, dehydrated in a graded ethanol/xylene series, embedded in paraffin, and cut into 5μm thick slices. The slices were then dewaxed for hematoxylin and eosin. Finally, the cells were examined under a light microscope.

Enzyme-linked immunosorbent assay (ELISA)

The levels of interleukin (IL)-4, IL-10, IL-6, IL-12, IL-1β, tumor necrosis factor-α (TNF-α), monocyte chemoattractant protein-1 (MCP-1), vascular endothelial growth factor (VEGF), and erythropoietin (EPO) in the serum and bone marrow were measured using ELISA kits. The IL-4 ELISA kits (ZC-37986, ZCi Bio, China), IL-6 ELISA kits (ZC-32446, ZCi Bio, China), IL-10 ELISA kits (ZC-37962, ZCi Bio, China), IL-12 ELISA kits (ZC-37964, ZCi Bio, China), IL-1β ELISA kits (ZC-37974, ZCi Bio, China), TNF-α ELISA kits (ZC-35733, ZCi Bio, China), MCP-1 ELISA kits (ZC-38075, ZCi Bio, China), EPO ELISA kits (ZC-38240, ZCi Bio, China), and VEGF ELISA kits (ZC-38845, ZCi Bio, China) were used. The experimental procedures were performed in accordance with the manufacturer's instructions.

Real-time fluorescence quantitative PCR

The total RNA from the bone marrow of mice was extracted using TRIzol reagent (Invitrogen, USA). The quantification of gene expression for HIF-1α, p65, and IκBα was carried out using SYBR Green assay (Vazyme, China) according to the manufacturer's instructions. Gene expression levels were quantified using the $2^{-\Delta\Delta Ct}$ method. The primers used were as follows: p65 forward primer:5'- CTC CAG GCT CCT GTT CGA GTC TCC AT-3; p65 reverse primer:5'- GTG GCG ATC ATC TGT GTC TGG CAA GT-3; HIF-1α forward primer:5'- TCA CTG CCA CTG CCA CCA CAA CTG-3'; HIF-1α reverse primer:5'- TCC GAC TGT GAG TGC CAC TGT ATG C-3'; IκBα forward primer:5'- CCA TGA AGG ACG AGG AGT ACG AGC AA-3'; IκBα reverse primer:5'- GAT CAC AGC CAA GTG GAG TGG AGT CT-3 β-actin served as a control. RT-qPCR was performed at 95°C for 10 min, followed by 40 cycles of 95°C for 2 s and 60°C for 30 s. The Melting curve analysis was performed at 95°C for 30 s, 60°C for 30 min, and 95°C for 30 s.

Western blotting (WB)

Bone marrow lysates were prepared using RIPA cell lysis buffer, and the supernatants were collected after 12000 rpm centrifugation for 15 min at 4°C. The total protein was measured using a BCA kit (Thermo Scientific, Rockford, IL, USA). From the supernatant sample 20μg were separated using sodium dodecyl sulfate-polyacrylamide gel electrophoresis (SDS-PAGE) and transferred onto PVDF membranes. The membrane was then blocked in TBS-T for 2 h at room temperature and washed three times by PBS. The immunoblots were incubated with primary antibodies overnight at 4°C. The primary antibodies were against HIF-1α (1:2000; no. A7684, Abclonal), p-65 (1:2000; no. Ab140751, Abcam), p-p65 (1:2000; no. Ab86299, Abcam), IκBα (1:5000; no. Ab32518, Abcam), and p-IκBα (1:5000; no. Ab133462, Abcam). The membrane was then incubated with secondary antibodies for 2 h at room temperature, washed again, and detected with ECL. Band sizes were quantified using Scion Image 4.0 software (Scion Corporation, Frederick, MD, USA). Sample loading was normalized relative to β-actin (1:100000; no. AC026; Abclonal) which was used as the reference standard.

Statistical analysis

GraphPad Prism 9.1.2 (GraphPad Software, Inc.) was used to analyze the data and generate the charts in this experiment. All data are presented

as the mean ± standard deviation, and all tests were performed at least three times. Unpaired t-test was used to analyze the differences between the two groups. Differences among the three groups were analyzed by one-way analysis of variance (ANOVA) for all experiments. Statistically significance was set at P < 0.05.

RESULTS

The effect of the administration of different doses and methods of busulfan on hemocyte levels in mice

The mice in the control group were in a nice psychiatric condition and had smooth coats, while the model mice were depressed and had bowed backs, dull coats, and low physical activity. To discover the best modeling methods, mice were treated with different doses and durations of busulfan treatment. After modeling, the mortality rates in each group were as follows:

AA-A1 (16.7%), AA-A2 (33.33%), AA-A3 (50%), AA-B1 (50%), AA-B2 (66.7%), and AA-B3 (83%). As shown in Figure 1, compared with the control group, the AA-B3 group (40 mg/kg/d, 10 days) showed the lowest levels of HGB, WBC, RBC, and PLT on day 10.

The effect of administration of different doses and methods of busulfan on the pathological change of bone marrow

To count nucleated cells, bone marrow smears were stained with Giemsa (Figure 2a). The results indicated that busulfan significantly decreased the number of nucleated cells in the bone marrow in a dose- and time-dependent manner. Hematoxylin and eosin staining was performed to observe pathological changes in mice. As shown in Figure 2b, the number of adipocytes in the femur marrow cavity increased with increasing busulfan dose and treatment time. Meanwhile, there was a reduction in the number
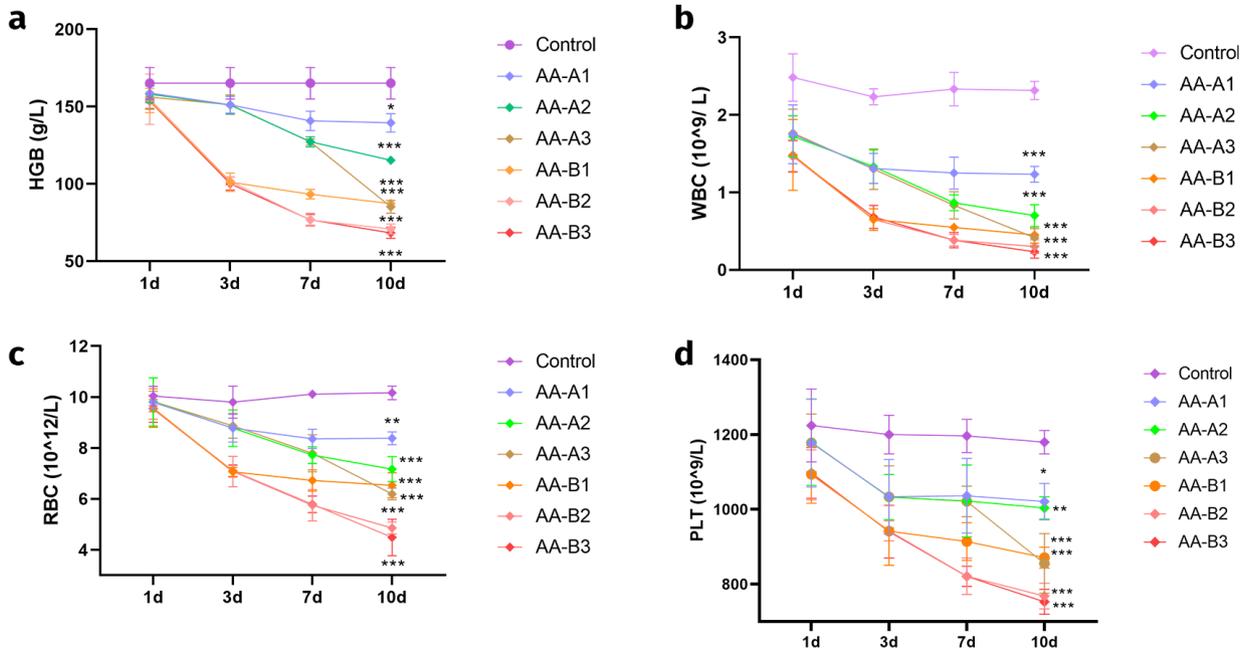

Figure 1. Hemocyte levels in mice following administration of different doses and methods of busulfan. Mice (n=3) were treated with 20mg/kg/d, 40mg/kg/d of busulfan for 5, 7, 10 days, respectively, busulfan was replaced by saline when treatment less than 10 days. Peripheral blood was collected on days 1, 3, 5, 7, 10. a. HGB content b. WBC content c. RBC content d. PLT content. Data are presented as means ± SD. *P < 0.05, **P < 0.01, ***P < 0.001 compared with control group.

of bone marrow cells and megakaryocytes. The phenomenon of dilated and congested blood sinusoids was most serious when the mice were treated with 40 mg/kg/d for 10 days.

Effects of RGP on hemocyte levels of AA mice

AA model mice were treated with 20 mg/kg/d busulfan for 10 days. 0.1mL of RGP (500 mg/mL), CA (5 mg/mL), or RGP (500 mg/mL) + CA (5 mg/mL) was administered to AA model mice twice daily for 10d. As shown in Figure 3a-d, compared with the control group, RBC (Figure 3a), PLT (Figure 3b), HGB (Figure 3c), and WBC (Figure 3d) were significantly decreased by busulfan, and this state was reversed by RGP. Additionally, the combination of cyclosporine and RGP resulted in better treatment.

Effects of RGP on the pathological change of the bone marrow of AA mice

To detect the effects of RGP on pathological changes in the bone marrow of AA mice, we performed Giemsa staining of the sternum marrow and HE staining of the right femur of mice after RGP and CA treatment. Figure 3e suggests that when RGP was combined with CA, there was a greater increase in nucleated cells compared with the other single drug treatment groups. Furthermore, as Figure 3f shows, compared with the AA group, three groups (AA+RGP, AA+CA, AA+RGP+CA) displayed an increased number of bone marrow cells and megakaryocytes, a reduced number of adipocytes, and dilated and congested blood sinusoids. The AA+RGP+CA group showed the closest pathological morphology to that of the control group.
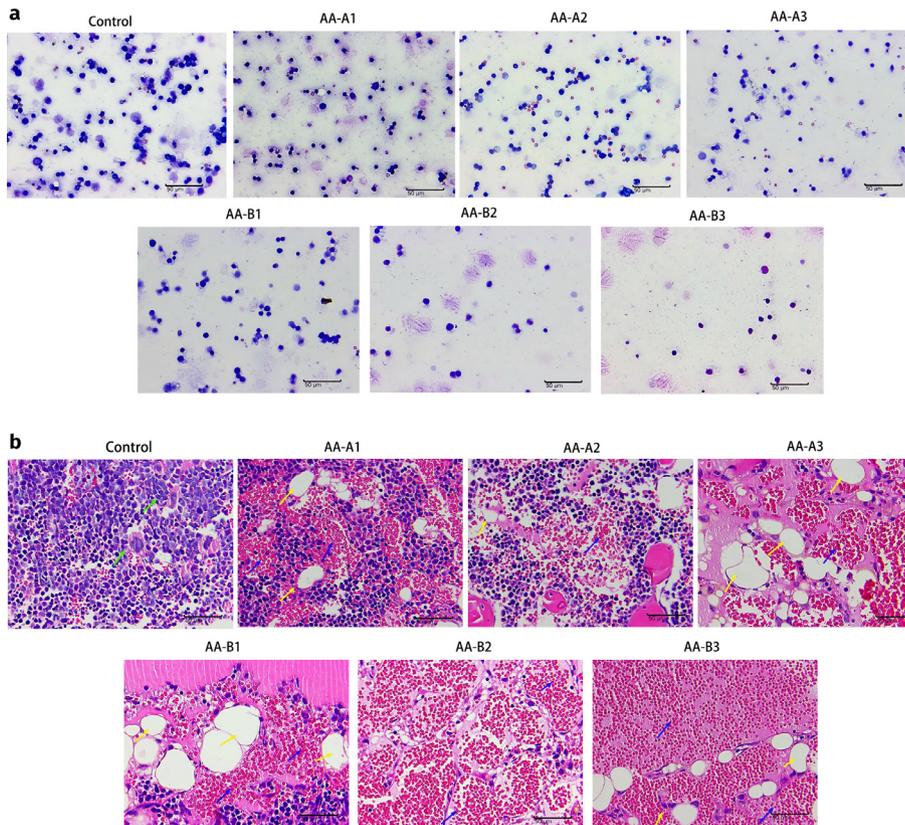

Figure 2. Pathological change in mice following administration of different doses and methods of busulfan. Mice (n=3) were treated with 20mg/kg/d, 40mg/kg/d of busulfan for 5, 7, 10 days, respectively, busulfan was replaced by saline when treatment less than 10 days. Peripheral blood was collected on days 1, 3, 5, 7, 10. a. Ray's Giemsa staining of sternum marrow. b. HE staining of the right femur. Adipocyte (yellow arrow), blood sinusoids dilated and congested (blue arrow), megakaryocyte (green arrow).
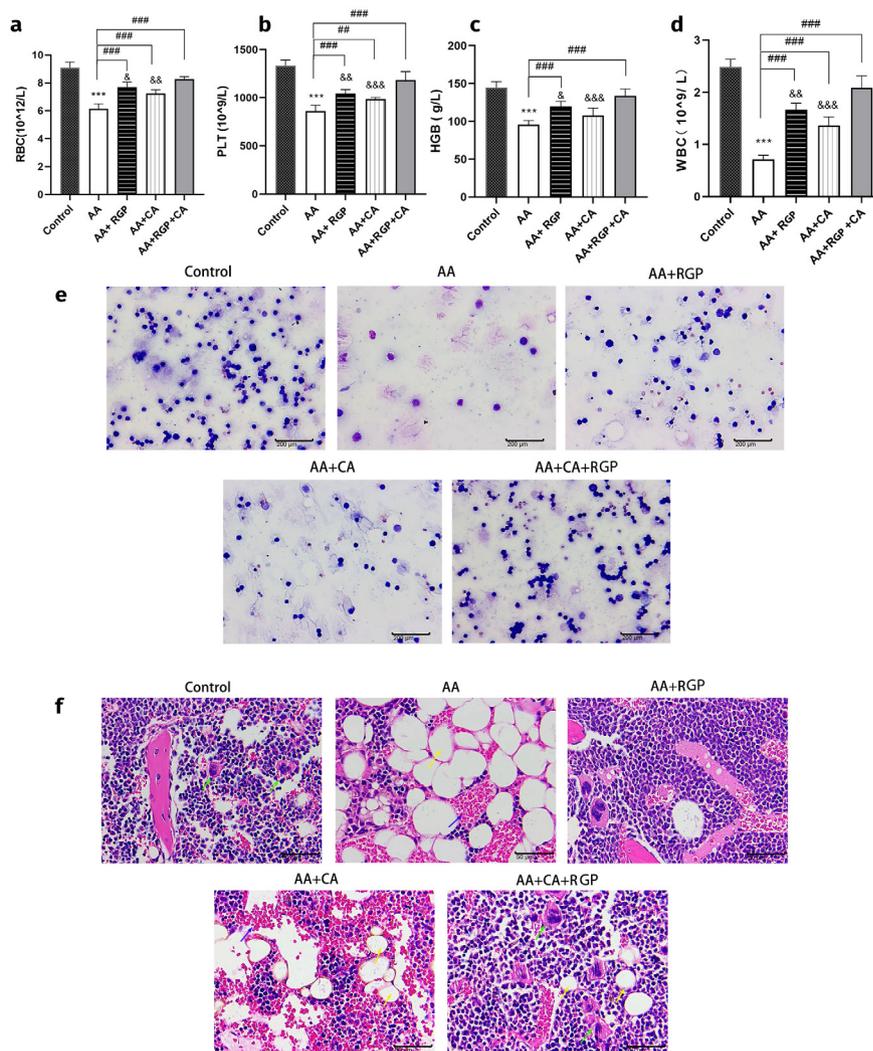
Figure 3. Effects of RGP on AA mice. a. HGB content b. WBC content c. RBC content d. PLT content. Data are presented as means ± SD. ***P < 0.001 compared with control group; ##P < 0.01, ###P < 0.001, compared with AA group; &&P < 0.01, &&&P < 0.001, compared with AA+ RGP +CA group. e. Ray's Giemsa staining of sternum marrow. f. HE staining of the right femur. Adipocyte (yellow arrow), blood sinusoids dilated and congested (blue arrow), megakaryocyte (green arrow).

Effects of RGP on inflammatory cytokines of AA mice

To assess the impact of RGP on the regulation of the bone marrow microenvironment, we performed ELISA to measure inflammatory cytokines in the bone marrow and blood. These cytokines included IL-4, IL-10, IL-6, IL-12, TNF-α, IL-1β, and MCP-1. As shown in Figure 4 (a-i), busulfan-induced expression of IL-6, IL-12, TNF-α, IL-1β, and MCP-1 was inhibited, and IL-4 and IL-10 were promoted by RGP in the blood of mice. Cyclosporin combined with RGP presented the best treatment compared with a single drug. Meanwhile, these cytokines in the bone marrow showed a similar trend (Figure 5a-i).

Effects of RGP on EPO and VEGF of AA mice

EPO and VEGF are two important factors associated with AA. Thus, we performed an ELISA to measure the expression of EPO and VEGF. The results indicated that VEGF expression either in the blood or bone marrow was downregulated by busulfan, and RGP reversed this effect (Figure 4h/ Figure 5h). Moreover, EPO expression in both blood and bone marrow was upregulated by busulfan and reversed by RGP (Figure 4i/ Figure 5i). However, RGP was more effective when administered in combination with cyclosporine.
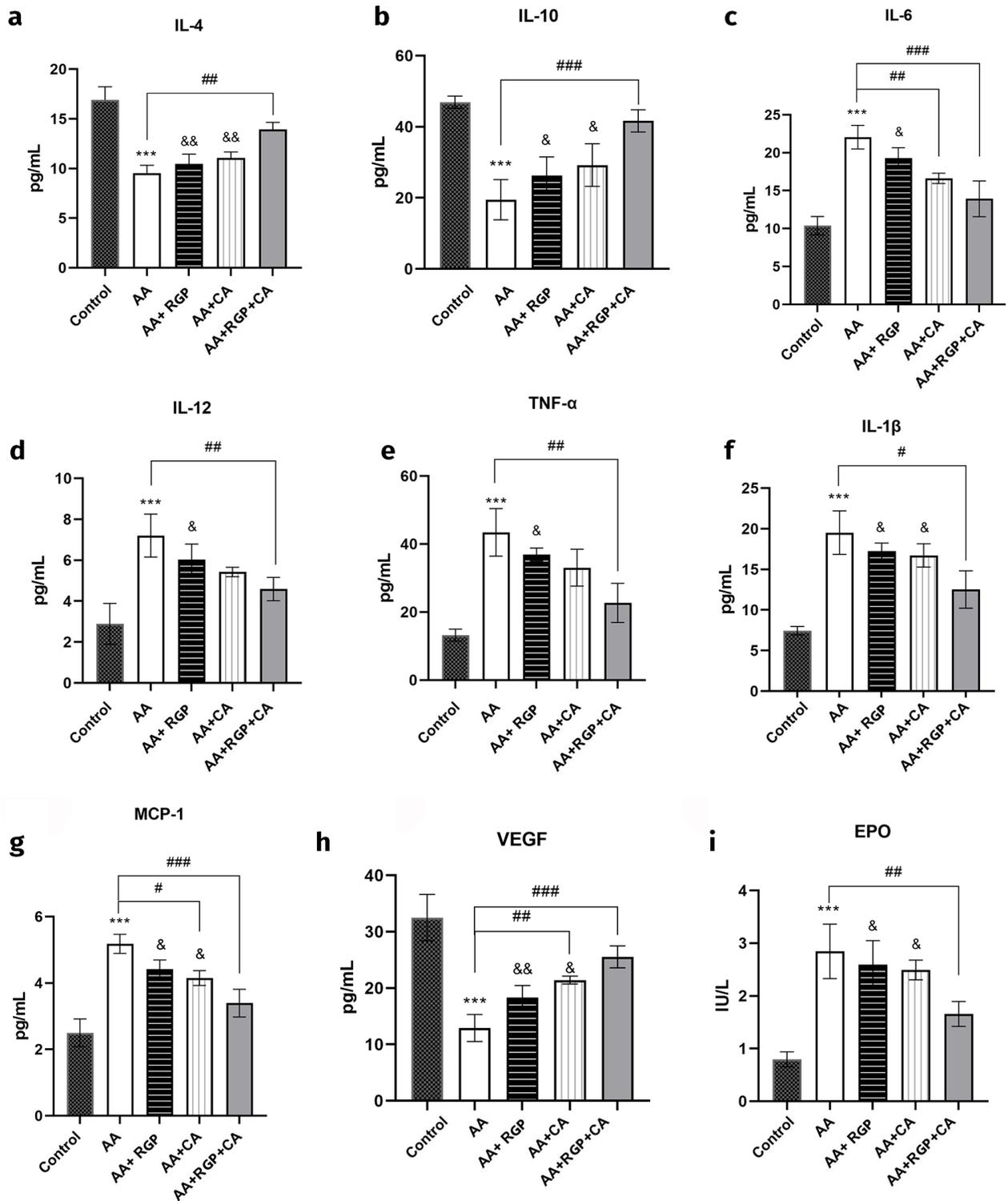
Figure 4. Effects of RGP on blood microenvironment. IL-4 (a), IL-10 (b), IL-6 (c), IL-12 (d), TNF-α (e), IL-1β (f), MCP-1 (g), VEGF (h), EPO (I) levels. Data are presented as means ± SD. ***P < 0.001 compared with control group; #P < 0.05, ##P < 0.01, ###P < 0.001, compared with AA group; &P < 0.05, &&P < 0.01, compared with AA+ RGP +CA group.
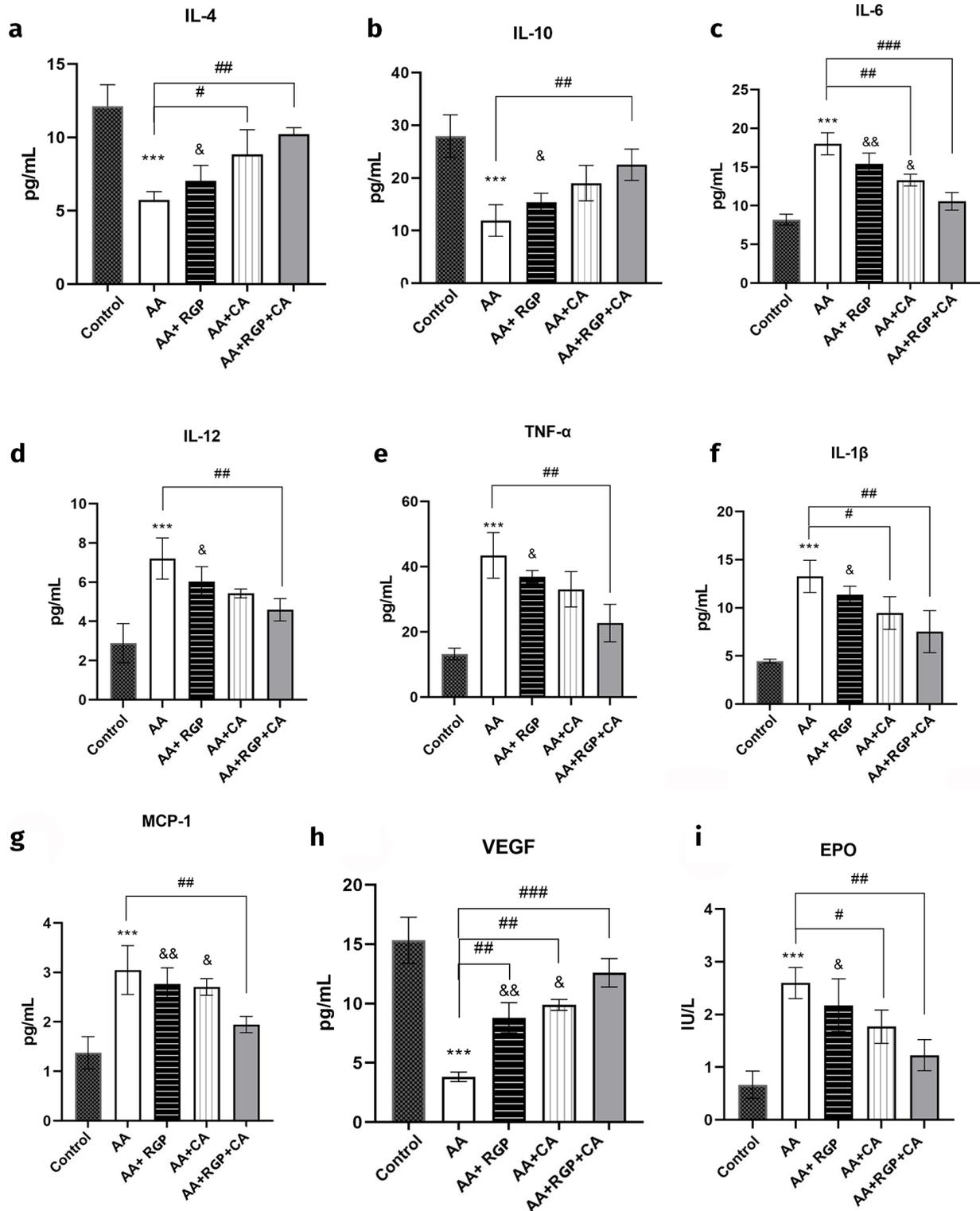
Figure 5. Effects of RGP on bone marrow microenvironment. Effects of prepared Rehmannia root polysaccharide on bone marrow inflammatory cytokine levels and MCP-1, EPO, VEGF2 levels. IL-4 (a), IL-10 (b), IL-6 (c), IL-12 (d), TNF-α (e), IL-1β (f), MCP-1 (g), VEGF (h), EPO (i) levels. Data are presented as means ± SD. ***P < 0.001 compared with control group; #P < 0.05, ##P < 0.01, ###P < 0.001, compared with AA group; &P < 0.05, &&P < 0.01, compared with AA+RGP+CA group.

Effects of RGP on HIF-1α/NF-κB signaling pathway

To explore the effects of RGP on the HIF-1α/NF-κB signaling pathway, the expression of proteins in the HIF-1α/NF-κB signaling pathway was analyzed. RT-qPCR analysis of HIF-1α, p65 e IκBα expression levels (Figure 6a). Busulfan-induced expression of HIF-1α, p-p65, and p-IκBα was inhibited. WB analysis for p-p65/p65, p-IκBα/IκBα ratio, and HIF-1α expression (Figure 6b-e). The p-p65/p65 ratio (Figure 6c), p-IκBα/IκBα ratio (Figure 6d), and HIF-1α level (Figure 6e) showed a similar trend: they were inhibited by cyclosporin and RGP, and their combination was more effective than the separate use. Therefore, RGP downregulated the activation of the HIF-1α/NF-κB signaling pathway.

DISCUSSION

Altered BMM is an important cause of AA. The variations in BMM include bone marrow microcirculation, cytokines, and interstitial cells (Xiong et al. 2015). Considering the functions of RGP and busulfan. This study investigated the influence of RGP on busulfan-induced changes in AA and BMM. The results showed that RGP inhibited busulfan-induced AA by suppressing the HIF-1α/NF-κB pathway in BALB/c mice.

Various AA modelling methods have been reported, such as benzene feeding, total-body irradiation, allogeneic lymphocyte infusion combination, heterogeneous lymphocyte implantation, and busulfan feeding (He et al. 2020, Mu et al. 2021, Zheng et al. 2019). Among them, busulfan is a bifunctional alkylating agent that is highly virulent for hematopoietic progenitor cells and HSCs and is commonly used in clinical practice for bone marrow transplantation and anti-tumor treatment (Bartelink et al. 2016). Busulfan-induced aplastic anemia in animals was first studied in 1974 (Santos & Tutschka 1974). AA modeling was further optimized in this study using different doses of busulfan feeding for different durations. We found that feeding mice 20 mg/kg/d busulfan for 10 days was an optimum modeling method.

Changes in the M1/M2 macrophage ratio and IFN-γand TNF-α levels have been reported to lead to AA (Mu et al. 2021). M1-type macrophages are recognized by Toll-like receptors (TLRs) and secrete pro-inflammatory factors, such as IL-6, IL-12, and TNF-α, which promote inflammation progression (Weisser et al. 2013). In contrast, M2-type macrophages are recognized by IL-10, IL-4, or TGF-β and secrete Arginase-1 (Arg-1) to inhibit inflammation progression (Gordon & Martinez 2010). In this study, we found that busulfan induced the expression of cytokines IL-4, IL-10, and VEGF down-regulation significantly, and upregulated the expression of IL-6, IL-12, TNF-α, MCP-1, IL-1β, and EPO. Our findings were consistent with this theory. Meanwhile, the quantities of HGB, WBC, RBC, and PLT were also significantly reduced. Furthermore, busulfan induced lipogenic differentiation and bone marrow sinus dilation. Adipocytes play a negative regulatory role in the differentiation and maturation of HSCs (Sarugaser et al. 2009). The number of adipocytes increases and that of hemocytes decreases whith AA occurrence (Chattopadhyay & Law 2020). This indicates that busulfan causes inflammation and impairs hematopoietic function. These cases were both dose-and time-dependent on busulfan administration. However, these events were reversed by RGP, indicating that RGP could be a potential candidate for AA treatment.

In recent years, except for RGP, other herbal active ingredients have therapeutic effects on AA, such as Dioscorea nipponica Makino and Tripterygium wilfordii polyside (Le 2019), Shenyubuxue prescription (Deng 2018). As Zhang Le reported, D. nipponica Makino
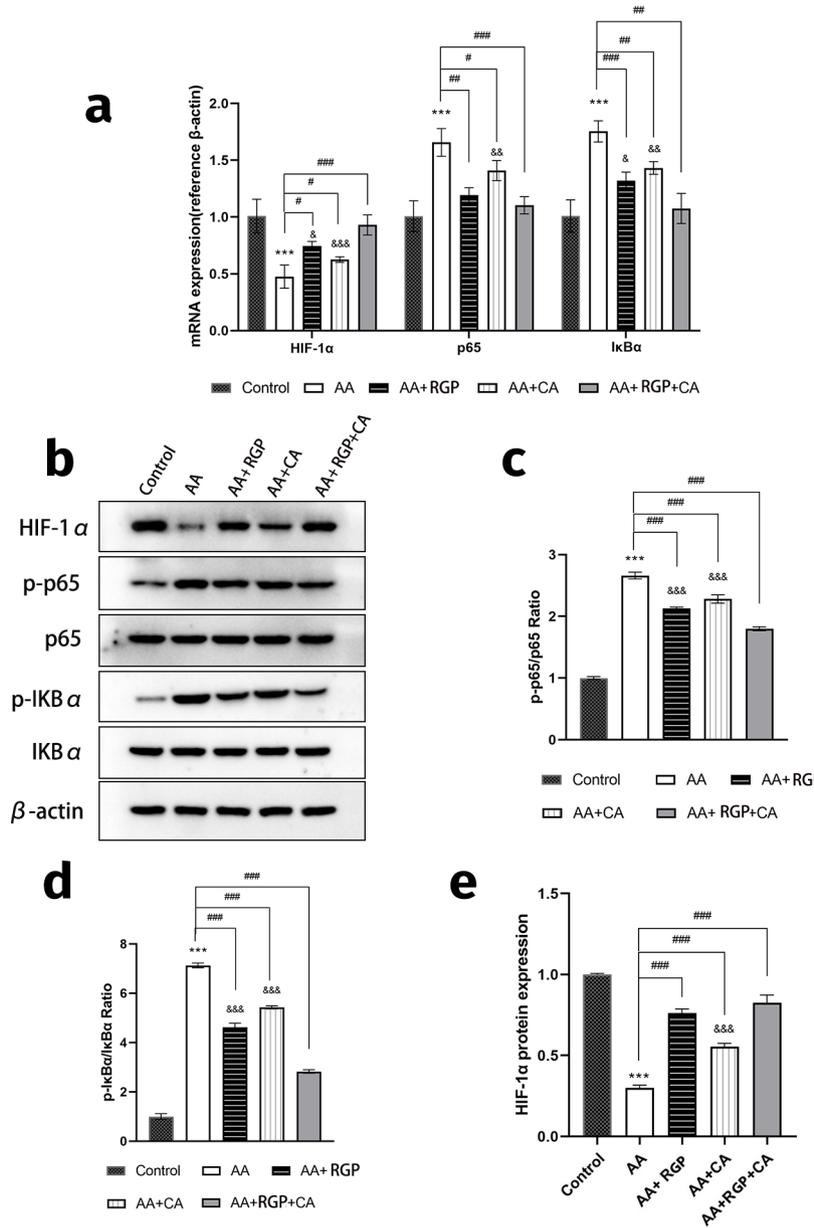
Figure 6. Effects of RGP on HIF-1α/NF-κB signaling pathway. a. The mRNA levels of HIF-1α, p65 e IκBα were analyzed by qRT-PCR. b. Protein bands of HIF-1α, p65, p-p65, IκBα, and p-IκBα were analyzed by WB. c. Analysis of p-p65/p65 ratio. d. Analysis of p-IκBα/ IκBα ratio. e. Analysis of HIF-1α. Data are presented as means ± SD. ***P < 0.001 compared with control group; #P < 0.05, ##P < 0.01, ###P < 0.001, compared with AA group; &P < 0.05, &&P < 0.01, &&&P < 0.001, compared with AA+ RGP +CA group.

inhibits the expression of HIF-1α and NF-kB in the bone marrow, increases the expression of IL-1β, and decreases TNF-α in AA mice (Le 2019). This suggests that the HIF-1α/NF-kB signaling pathway might be a new target for controlling AA. Activation of the NF-κB signaling pathway is controlled by p65 and IκBα phosphorylation (Baldwin 1996). In this study, we found that the phosphorylation of IκBα and p-65 was inhibited by RGP, while busulfan activated it. These results are consistent with those of previous studies. RGP and CA have similar pharmacological effects, and the results demonstrate that RGP provides synergistic effects with CA. In summary, this study provides an excellent reference for the clinical use of AA.

CONCLUSIONS

This study enumerated a traditional Chinese medicine to control AA and illustrated the key role of the HIF-1α/NF-κB signaling pathway in the process of AA. Moreover, RGP suppressed busulfan-induced AA by suppressing the HIF-1α/NF-κB signaling pathway in vivo. This study provides a reference for the treatment of AA and the development of therapeutic drugs. Nevertheless, the effect of RGP on busulfan-induced AA needs to be studied in vivo in the future.

Acknowledgments

REFERENCES

BALDWIN AS JR. 1996. The NF-kappa B and I kappa B proteins: new discoveries and insights. Annu Rev Immunol 14: 649-683.

BARTELINK IH ET AL. 2016. Association of busulfan exposure with survival and toxicity after haemopoietic cell transplantation in children and young adults: a multicentre, retrospective cohort analysis. Lancet Haematol 3: e526-e536.

CHATTOPADHYAY S & LAW S. 2020. Morphogen signaling by Wnt/beta-catenin pathway and microenvironmental alteration in the bone marrow of agricultural pesticide exposure-induced experimental aplastic anemia. J Biochem Mol Toxicol: e22523.

DASOUKI MJ, RAFI SK, OLM-SHIPMAN AJ, WILSON NR, ABHYANKAR S, GANTER B, FURNESS LM, FANG J, CALADO RT & SAADI I. 2013. Exome sequencing reveals a thrombopoietin ligand mutation in a Micronesian family with autosomal recessive aplastic anemia. Blood 122: 3440-3449.

DENG D. 2018. clincal reseach on the effect of shenyubuxue prescription combined withCSAin treating spleen-kidney yang deficiency chronic aplastic anemia. D, Guangxi University of Chinese Medicine.

FENG T & WU QF. 2022. A review of non-coding RNA related to NF-kappaB signaling pathway in the pathogenesis of osteoarthritis. Int Immunopharmacol 106: 108607.

GONG W, ZHANG N, CHENG G, ZHANG Q, HE Y, SHEN Y, ZHANG Q, ZHU B, ZHANG Q & QIN L. 2019. Rehmannia glutinosa Libosch Extracts Prevent Bone Loss and Architectural Deterioration and Enhance Osteoblastic Bone Formation by Regulating the IGF-1/PI3K/mTOR Pathway in Streptozotocin-Induced Diabetic Rats. Int J Mol Sci 20.

GORDON S & MARTINEZ FO. 2010. Alternative activation of macrophages: mechanism and functions. Immunity 32: 593-604.

HE J, HAN R, YU G, LAVIN MF, JIA Q, CUI P & PENG C. 2020. Epimedium Polysaccharide Ameliorates Benzene-Induced Aplastic Anemia in Mice. Evid Based Complement Alternat Med 2020: 5637507.

HUANG Y, NAN L, XIAO C, JI Q, LI K, WEI Q, LIU Y & BAO G. 2019. Optimum Preparation Method for Self-Assembled PEGylation Nano-Adjuvant Based on Rehmannia glutinosa Polysaccharide and Its Immunological Effect on Macrophages. Int J Nanomedicine 14: 9361-9375.

KIHO T, WATANABE T, NAGAI K & UKAI S. 1992. Hypoglycemic activity of polysaccharide fraction from rhizome of Rehmannia glutinosa Libosch. f. hueichingensis Hsiao and the effect on carbohydrate metabolism in normal mouse liver]. Yakugaku Zasshi 112: 393-400.

KILLICK SB ET AL. 2016. Guidelines for the diagnosis and management of adult aplastic anaemia. Br J Haematol 172: 187-207.

LE Z. 2019. Study on the mechanism of treatment of aplastic anwmia throuh the HIF-1α/NF-κB pathway by dioscorea nipponica makino. D, Tianjin Medical University.

LI J ET AL. 2012. Differential gene expression profile associated with the abnormality of bone marrow mesenchymal stem cells in aplastic anemia. PLoS One 7: e47764.

LIU HY & LIU TT. 2015. [Research Progress on Pathogenesis of Aplastic Anemia]. Zhongguo Shi Yan Xue Ye Xue Za Zhi 23: 1216-1220.

MU H, JIA H, LIN ZH, ZHENG HH, WANG L & LIU H. 2021. [Role of imbalance of M1/M2 subsets of bone marrow macrophages in the pathogenesis of immune-mediated aplastic anemia in mice]. Zhonghua Xue Ye Xue Za Zhi 42: 945-951.

NUTTALL ME & GIMBLE JM. 2004. Controlling the balance between osteoblastogenesis and adipogenesis and the consequent therapeutic implications. Curr Opin Pharmacol 4: 290-294.

POLINENI S, RESULAJ M, FAJE AT, MEENAGHAN E, BREDELLA MA, BOUXSEIN M, LEE H, MACDOUGALD OA, KLIBANSKI A & FAZELI PK. 2020. Red and White Blood Cell Counts Are Associated With Bone Marrow Adipose Tissue, Bone Mineral Density, and Bone Microarchitecture in Premenopausal Women. J Bone Miner Res 35: 1031-1039.

SANTOS GW & TUTSCHKA PJ. 1974. Marrow transplantation in the busulfan-treated rat: preclinical model of aplastic anemia. J Natl Cancer Inst 53: 1781-1785.

SARUGASER R, HANOUN L, KEATING A, STANFORD WL & DAVIES JE. 2009. Human mesenchymal stem cells self-renew and differentiate according to a deterministic hierarchy. PLoS One 4: e6498.

SIVASUBRAMANIYAN K ET AL. 2012. Phenotypic and functional heterogeneity of human bone marrow- and amnion-derived MSC subsets. Ann N Y Acad Sci 1266: 94-106.

SOLOMOU EE, REZVANI K, MIELKE S, MALIDE D, KEYVANFAR K, VISCONTE V, KAJIGAYA S, BARRETT AJ & YOUNG NS. 2007. Deficient CD4+ CD25+ FOXP3+ T regulatory cells in acquired aplastic anemia. Blood 110: 1603-1606.

USMANI S, SIVAGNANALINGAM U, TKACHENKO O, NUNEZ L, SHAND JC & MULLEN CA. 2019. Support of acute lymphoblastic leukemia cells by nonmalignant bone marrow stromal cells. Oncol Lett 17: 5039-5049.

WANG J, WENG Y, ZHANG M, LI Y, FAN M, GUO Y, SUN Y, LI W & SHI Q. 2016. BMP9 inhibits the growth and migration of lung adenocarcinoma A549 cells in a bone marrow stromal cellderived microenvironment through the MAPK/ERK and NF-kappaB pathways. Oncol Rep 36: 410-418.

WANG ZL & LI L. 1997. Effects of Radix Rehmanniae on gastric acid secretion and gastric ulcer formation in rats. World J Gastroenterol 3: 197.

WEISSER SB, MCLARREN KW, KURODA E & SLY LM. 2013. Generation and characterization of murine alternatively activated macrophages. Methods Mol Biol 946: 225-239.

XIONG H, YANG XY, HAN J, WANG Q & ZOU ZL. 2015. Cytokine expression patterns and mesenchymal stem cell karyotypes from the bone marrow microenvironment of patients with myelodysplastic syndromes. Braz J Med Biol Res 48: 207-213.

XU L, ZHANG W, ZENG L & JIN JO. 2017. Rehmannia glutinosa polysaccharide induced an anti-cancer effect by activating natural killer cells. Int J Biol Macromol 105: 680-685.

YOUNG NS. 2013. Current concepts in the pathophysiology and treatment of aplastic anemia. Hematology Am Soc Hematol Educ Program 2013: 76-81.

YOUNG NS, BACIGALUPO A & MARSH JC. 2010. Aplastic anemia: pathophysiology and treatment. Biol Blood Marrow Transplant 16: S119-125.

YOUNG NS, CALADO RT & SCHEINBERG P. 2006. Current concepts in the pathophysiology and treatment of aplastic anemia. Blood 108: 2509-2519.

ZHENG ZY, YU XL, DAI TY, YIN LM, ZHAO YN, XU M, ZHUANG HF, CHONG BH & GAO RL. 2019. Panaxdiol Saponins Component Promotes Hematopoiesis and Modulates T Lymphocyte Dysregulation in Aplastic Anemia Model Mice. Chin J Integr Med 25: 902-910.

NA LIU[1#]
https://orcid.org/0000-0001-7704-8123

JUN-QIU LIU[2#]
https://orcid.org/0000-0001-5953-2026

YONG LIU[1]
https://orcid.org/0009-0005-6446-3404

QING ZHU[1]
https://orcid.org/0009-0001-7039-5699

DANDAN ZHENG[1]
https://orcid.org/0009-0005-6354-6101

FENG LI[1]
https://orcid.org/0009-0001-6718-8955

LING-ZHAN MENG[1]
https://orcid.org/0000-0002-7861-8017

MIN QIU[1]
https://orcid.org/0009-0007-7534-2012

[1]Chongqing Hospital of Traditional Chinese Medicine, Department of Oncology, No.6, Panxi Seventh Branch Road, Jiangbei District, Chongqing, 400021, China

[2]Zhejiang Chinese Medical University, School of Pharmaceutical Science, No. 548, Binwen Road, Binjiang District, Hangzhou, Zhejiang Province, 311402, China

Correspondence to: **Min Qiu**
E-mail: liunach2022@163.com

[#]Co-first authors

Author contributions

Conceptualization: Na Liu, Jun-qiu Liu and Min Qiu. Formal analysis and investigation: Yong Liu and Qing Zhu. Methodology: Dandan Zheng and Feng Li. Writing-original draft preparation: Min Qiu. Writing-review and editing: Na Liu and Jun-Qiu Liu. Supervision: Ling-zhan Meng. All authors gave final approval, and agreed to be accountable for all aspects of the work ensuring integrity and accuracy.